

# **Femtosecond Pulse Shaping With Spatial–Light Modulator Based On Twist Nematic With Homeotropic Boundary Conditions**

A.P. Grigoryan, M.R. Hakobyan, R.S. Hakobyan\*

*Physics Department, Yerevan State University, 1 Alex Manoogian, 0025 Yerevan, Armenia*

\*e-mail: rhakob@ysu.am

Received 27 November 2017

**Abstract:** The possibility of femtosecond optical pulses shaping using a spatial–light modulator (SLM) based on the twisted nematic (TN) liquid crystal with homeotropic boundary conditions is theoretically considered. Phase sensitive pulse shaping using a TNSLM and the shaped waveforms are calculated. Using this kind of LC structure allows to control shaping process by electrical fields with voltages much less than 1V.

**Keywords:** pulse shaping, femtosecond, liquid crystal, spatial light modulator

## **1. Introduction**

In the last two decades, much attention has been paid to the development of a technique for the shaping and compression of femtosecond optical pulses using a grating-lens apparatus with a liquid crystal spatial light modulator (SLM) [1,2]. Such SLMs can independently control the amplitude and the phase of the transmitted light giving possibility to programmable generate pulses with practically arbitrary (within physical limits) shaping and are now commercially available. The commercial SLMs most often have a twisted nematic structure [3], and the amplitude and the phase of the transmitted light are coupled in a specific manner. That is why in [4] the authors focused on pulse shaping with such SLMs in the time domain and investigated the potential of the technique. In [5,6] we have considered the distribution of the director of a cholesteric liquid crystal (CLC) in planar cells on whose walls the director orientation is maintained rigidly along the normal to the boundary. This kind of structure has also twist nematic with cholesteric mixture (TNCM) and with homeotropic boundaries. Near the critical cell thickness, this system becomes sensitive to the external fields and at a very low electrical voltage, a transition of the Fréedericksz type takes place from a stable twisted distribution to a stable homogeneous homeotropic distribution.

In this study, we have theoretically characterized the properties of a TNCM SLM with homeotropic boundary conditions. We developed the relevant mode extraction method for the calculation of mask patterns, which can generate multiple pulse sequences with arbitrary relative amplitudes and phases. By the choosing relevant distribution of the electric field voltages (lower than 1V) across the mask with TNCM SLM we get very different pulse shaping. By varying the modulation depth (by altering the amplitude of the electric field voltages distribution), we generate different number of pulses and intensity ratio of them.

## 2. Liquid crystal modulator

The SLM consists of a TNCM or CLC layer, which is embedded between two glass slides. The TNCM mask is subdivided into a linear array of pixels, which can be controlled individually using a driving voltage. It is applied via two transparent indium tin oxide (ITO) electrodes which are deposited on the inner surface of the glass slides. The pixels are defined by patterning of one ITO layer into stripe-shaped electrodes, with neighboring pixels being separated by thin gaps (typically a few microns) in the ITO layer.

Generally for a birefringent material, the optical phase difference between extraordinary and ordinary waves with refractive indexes  $n_e$  and  $n_o$ , respectively, or retardance, is given as

$$\Delta\psi = \frac{2\pi L}{\lambda}(n_e - n_o), \quad (1)$$

where  $L$  is the thickness of the material and  $\lambda$  is the wavelength. The axes of liquid crystal modulator (LCM) pixels are defined as follows. The  $x$ -axis is directed along the spatial frequency spread, the  $y$ -axis is orthogonal to  $x$  and the direction of light propagation,  $z$ -axis. The unite vector  $\mathbf{n}$  describing preferred orientation of LC molecules is called director. Initial orientation of director  $\mathbf{n}$  in the every pixel cell has twisted structure [7]. At a cell thickness  $L_{cr} = K_3 P / 2K_2$ , where  $P$  is the pitch parameter of the free CLC or TNCM and  $K_i$  are Frank's elastic constants, a transition of the Fréedericksz type takes place from a stable homogeneous homeotropic distribution (for  $L < L_{cr}$ ) to a stable twisted distribution (for  $L > L_{cr}$ ) rotation angle  $\varphi(z) = 2\pi z / P$ . For twist nematic with cholesteric mixture  $\varphi(L) = \pi/2$ . In general, director distribution has the form

$$\mathbf{n} = (\mathbf{e}_x \cos \varphi + \mathbf{e}_y \sin \varphi) \sin \theta + \mathbf{e}_z \cos \theta, \quad (2)$$

where  $\mathbf{e}_i$  are orts of coordinate system, and  $\theta$  is the polar angle dependent only on  $z$ . Homeotropic boundary conditions mean that  $\theta(z=0, L) = 0$ . Above and very close to the critical thickness distribution of polar angle could be approximated as

$$\theta(z) = \theta_m \sin \frac{\pi z}{L}, \quad \sin \theta_m = (2K_2 L / K_3 P - 1)^{1/2}. \quad (3)$$

This director distribution could be controlled by electric or magnetic fields with very low threshold values near the critical thickness:

$$\frac{\varepsilon_a}{4\pi K_3} E_{cr} = \left( \frac{2\pi K_2}{K_3} \right)^2 - \left( \frac{\pi}{L} \right)^2 \quad \text{and} \quad \frac{\chi_a}{K_3} H_{cr} = \left( \frac{2\pi K_2}{K_3} \right)^2 - \left( \frac{\pi}{L} \right)^2, \quad (4)$$

where  $E$  and  $H$  are electric and magnetic field strengths,  $\varepsilon_a$  and  $\chi_a$  are electric and magnetic susceptibility anisotropies. We will work very close and above to the electric field threshold. The orientation of the LC molecules lies, mainly, in the plane parallel to the wall surfaces (expects, very

thin layers close to the walls where they are normal to them) when no voltage is applied, and is twisted from one surface to the other by an angle (twist angle) of around  $\phi$ . Very weak electrical field (less than 0.1V) reorients LC director to the  $z$ -axis direction, which results in a variable refraction index for light polarized along the  $\mathbf{n}_0$ -axis. However, for light polarized perpendicularly to the  $\mathbf{n}_0$ -axis the refraction index remains constant. Therefore, retardance (1) depends on electric field voltage  $V$ .

$$\Delta\psi(V) = \frac{2\pi L}{\lambda} \Delta n(V), \quad (5)$$

where  $\Delta n = n_e(V) - n_o$ . The polarization properties of light transmitted through a twist nematic is presented in [8]. The amplitude and the phase of the transmitted light through TNCM with homeotropic boundary conditions in the present polarization combination can be derived in a similar manner. The resulted complex transmission coefficient is

$$T(V) = \frac{\sin^2(\phi\sqrt{1+u^2})}{1+u^2} \exp\left(-i\frac{\pi u}{2}\right), \quad (6)$$

where  $u(V) = \Delta\psi(V)/\pi$  is the Mauguin parameter and the twist angle could be equal to  $\pi/2$ . Let us consider crossed polarizers before and after the mask. So,  $u$  can be changed from 0 (complete transmission) at the moderate voltage to  $\sqrt{3}$  (no transmission) without electrical field by changing the voltage applied to the LC.

### 3. Mask Pattern Design and Results

As it was mentioned above, the modulator consists of array of LC pixels. Due to the electrically variable birefringence of LC the transmission (6) for each pixel  $T_n = T(V_n)$  is also controllable. In order to impose each spectral component of ultrashort pulse to carry out own retardance one needs to image the focused spectrum onto the SLM mask. We consider the single mask. In this case the easiest realization is to use a pair of gratings and lenses configured in a 4-F arrangement [9], when two gratings and mask are placed exactly in the focuses of two lenses. The first lens collimates the spatially separated by first grating spectral components of ultrashort pulse and focuses the each spectral component onto the spatially varying mask placed in the front focal plane of the lens. The mask is in the back focal plane of a second lens (so that the lens pair forms a telescope around the mask), which collimates the each spectral component and curves them to the second grating that is in the front focal plane of the second lens. The second lens and the second grating thus recombine the spectrally filtered pulse, yielding a shaped pulse in the time domain.

Now we can write a masking filter  $M(x)$  including both the pixels and the gap responses [9]

$$M(x) = \delta(x - x_0) \otimes \sum_{n=-N/2}^{N/2-1} \left\{ [T_n \delta(x - na)] \otimes squ\left(\frac{x}{ra}\right) + [T_g \delta(x - (n+1/2)a)] \otimes squ(x/(1-r)a) \right\}, \quad (7)$$

where  $N$  is the total number of pixels per array,  $x_0$  is the displacement of the center of the middle pixel ( $n=0$ ) of the mask from the  $\omega = \omega_0$  central spectral component,  $T_n$  is the response for each pixel  $n$ ,  $T_g$  is the response for the gaps,  $a$  is the center to center pixel distance (including gaps),  $\delta(x)$  is the Dirac delta function,  $r$  is the pixel width divided by the pixel width plus the gap width,  $squ(x)$  is a function defined as

$$squ(x) = \begin{cases} 1 & |x| \leq 1/2 \\ 0 & |x| > 1/2 \end{cases}. \quad (8)$$

Note that  $T_i$  are necessarily less than or equal to 1. Sign  $\otimes$  means the convolution of two functions  $f(x)$  and  $g(x)$  to give  $h(x)$  is defined as

$$h(x) = f(x) \otimes g(x) = \int_{-\infty}^{\infty} dx' f(x-x') g(x'). \quad (9)$$

We take the effect of the gaps as 0 because our spot size at the modulator is much larger than the width of the gap (we take the ratio of 3:100), thus the convolution will “hide” these smaller term. Furthermore, given the dimensions of the LC modulator,  $r$  is equal to 97/100, which is approximately one. With these approximations, equation (7) can be written as

$$M(x) = \delta(x - x_0) \otimes \sum_{n=-N/2}^{N/2-1} \left\{ [B_n \delta(x - na)] \otimes squ\left(\frac{x}{ra}\right) \right\}. \quad (10)$$

Furthermore, the delta function convoluted with the sum, results in only a shift to  $x_0$ . Theoretically considering this equation, the shift is irrelevant because the center frequency can be set to the center pixel. Experimentally, it is also possible to set this condition. The further simplified equation becomes [9],

$$M(x) = \sum_{n=-N/2}^{N/2-1} \left\{ [B_n \delta(x - na)] \otimes squ\left(\frac{x}{a}\right) \right\}. \quad (11)$$

When the spot size,  $w_0$ , is smaller than the individual pixel width, the frequency filter becomes equivalent in form to the physical mask

$$M_{eff}(\omega) \sim M(x/a).$$

(12)

Now let us calculate the Fourier transformation of (7)  $M(k)$ . For simplicity we assume that the pattern defined by the  $N$  pixels of the SLM repeats infinitely for  $x \rightarrow \pm\infty$ . With this assumption,  $M(k)$  will be expressed by Fourier transformation of masking function when it is repeated infinitely. The result is

$$M(k) = \exp(ikx_0) \frac{\sin(rka)}{\pi k} \left[ \sum_{n=-\infty}^{\infty} (-1)^n \delta\left(k - n \frac{2\pi}{a}\right) \right] \times \left\{ \sum_{n=-\infty}^{\infty} T_{rem(n,N)} \delta\left(k - n \frac{2\pi}{na}\right) + B_g \frac{\sin((1-r)ka)}{\pi k} \right\}, \quad (13)$$

where  $rem(n, N)$  gives the remainder of  $n / N$  and  $T_n$  is given by (6). In the frequency domain, the output of the linear filter,  $E_{out}(\omega)$ , is the product of the input signal,  $E_{in}(\omega)$ , and the frequency response,  $H(\omega)$ ,

$$E_{out}(\omega) = H(\omega)E_{in}(\omega), \quad (14)$$

where  $E_{in}$  and are  $E_{out}$  complex amplitudes of the input and output electric field spectra, respectively. Furthermore, it should be noted that  $E_{in}(\omega)$ ,  $E_{out}(\omega)$  and  $H(\omega)$  and  $e_{in}(t)$ ,  $e_{out}(t)$  and  $h(t)$  are, respectively, Fourier transform pairs which are defined as

$$e(t) = \frac{1}{2\pi} \int_{-\infty}^{\infty} E(\omega) e^{-i\omega t} d\omega, \quad E(\omega) = \int_{-\infty}^{\infty} e(t) e^{i\omega t} dt, \quad (15)$$

$$h(t) = \frac{1}{2\pi} \int_{-\infty}^{\infty} H(\Omega) e^{-i\Omega t} d\Omega, \quad H(\Omega) = \int_{-\infty}^{\infty} h(t) e^{i\Omega t} dt, \quad (16)$$

$H(\omega)$  can also be called the effective frequency mask,  $M_{eff}(\omega)$ , which is related to the physical mask [1] by

$$H(\omega) = M_{eff}(\omega) = \int dx M(x) g(x, \omega). \quad (17)$$

The effective frequency filter is given by the complex transmittance of the physical mask,  $M(x)$ , convolved with the spatial intensity profile of the impingent beam,  $g(x)$ , which, for example, can be defined as

$$g(x, \omega) = \left( \frac{2}{\pi w_0^2} \right)^{1/2} e^{-2(x-\alpha\omega)^2/w_0^2} \quad (18)$$

for a Gaussian shape, and

$$w_0 = \frac{f \lambda \cos \theta_{in}}{\pi w_{in} \cos \theta_d} \quad (19)$$

is the radius of the focused spot at the masking plane, where  $\theta_{in}$  is the light incident angle, and  $w_{in}$  is the spot size before the grating. Combining the results of Eqs. (6), (7), (14), (15), (17) and solving the system by the simulated–annealing (SA) computer program [10] it could be find the pulse shaping due to the mask on the twist nematic with cholesteric mixture and with homeotropic boundaries. For calculations, consider mask pattern giving the pixel number dependence of Mauguin parameter  $u(n)$  shown in Fig. 1. This kind of TNCM SLM mask pattern generates the waveform shown in Fig. 2. The input pulse was assumed to be a 21 fs  $\text{sech}^2$  pulse with unit intensity. The simulated waveform obtained by SA calculation has a high peak at 132 fs at the positive time direction. There remains, however, a peak at time zero with a comparable intensity, and several small peaks are also apparent at the negative times of  $-132\text{fs}$ ,  $-264\text{fs}$  and  $-396\text{fs}$ . These peaks appear due to the coupling between the amplitude and phase of the shaping procedure.

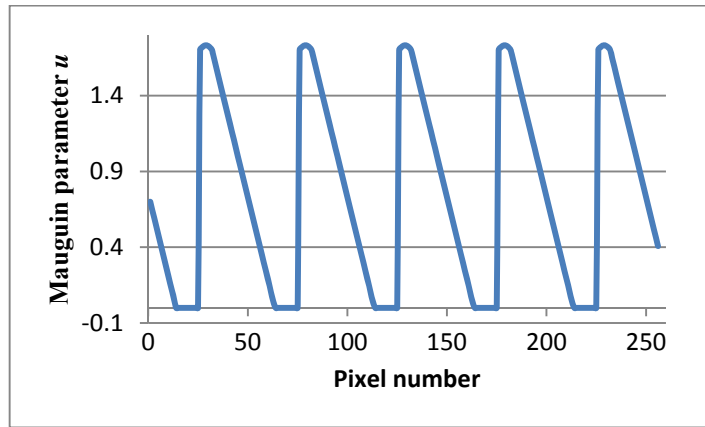


**Fig. 1.** SLM mask pattern which generates the waveform. The vertical axis shows the Mauguin parameter  $u$  of each pixel.

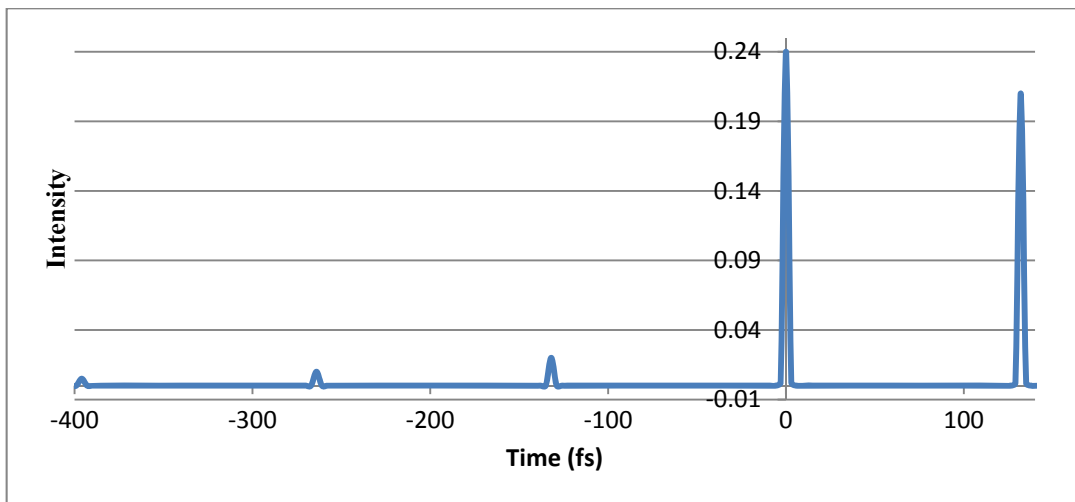


**Fig. 2.** Waveform with a single pulse at 132 fs in the positive time region obtained by a simulated annealing calculation. The peak intensity of the input pulse is normalized to unity.

Let us note some pixilation effects. Before voltage is applied on each pixel, all the LC molecules are aligned in the plane parallel to the cell walls, except those who are in the vicinity of the glass plates. This is because rigid homeotropic conditions on the walls. When the voltage is applied, the whole molecules are exactly aligned homeotropically and parallel to the field. If an exact pulse shape is desired the inhomogeneous distribution of molecules in the absence of electric field will bring to the observable imperfections between the desired and the measured shape.

#### **4. Conclusions**

Thus, we have developed the relevant mode extraction method for the calculation of mask patterns, which can generate multiple pulse sequences with arbitrary relative amplitudes and phases. We used SLM on the base of twist nematic with cholesteric mixture and with homeotropic boundary conditions. By the choosing relevant distribution of the electric field voltages ( $\sim 0.1$  V) across the mask with SLM we get very different pulse shaping. This approach allows to control of the relative amplitudes of different pulse within pulse train. By varying the modulation depth (by altering the amplitude of the electric field voltages distribution), we generate different number of pulses and intensity ratio of them. Electric field used energy could be made much lower by mixing ferroelectric nanoparticles with LC. It is well known [11,12,13] that ferroelectric nanoparticles could produce enhanced changes in the physical properties of LC host. Electrical Fréedericksz transition in twist nematic with cholesteric mixture doped with spherical ferroelectric nanoparticles has very low threshold because they strongly increase the electric field in the medium.

#### **Acknowledgments**

This work was supported by the RA MES State Committee of Science, in the frames of the research project № 15T-1C099.

#### **References**

- [1] A.M. Weiner, Review of Scientific Instruments, **71**(5), 1929 (2000).
- [2] B. Sun, P.S. Salter, M.J. Booth, Optics Express, **23**(15), 19348 (2015).
- [3] M.R. Hakobyan, R.S. Hakobyan, Armenian Journal of Physics, **7**(2), 59 (2014).
- [4] T. Hattori, K. Kabuki, Y. Kawashima, M. Daikoku, H. Nakatsuka, Jpn. J. Appl. Phys., **38**, 5898 (1999).
- [5] R.S. Akopyan, R.B. Alaverdyan, V.V. Saakyan, Yu.S. Chilingaryan, Kristallografiya, **30**(4), 746 (1985).
- [6] R.S. Akopyan, R.B. Alaverdyan, Yu.S. Chilingaryan, Sov. Journ. Contemp. Phys. (Arm. Ac. Sc.), **21**(4), 77 (1986).
- [7] B.Ya. Zeldovich, N.V. Tabiryan, Sov. Phys. JETP, **56**(3), 563 (1982).
- [8] P. Yeh, C. Gu. Optics of Liquid Crystal Displays. John Wiley & Sons, Inc., Hoboken, New Jersey, USA, 2010.
- [9] M.M. Wefers, K.A. Nelson, J. Opt. Soc. Am. B, **12**(7), 1343 (1995).
- [10] W.H. Press, S.A. Teukolsky, W.T. Vetterling, B.P. Flannery. Numerical Recipes. Cambridge University Press, Cambridge, 1992, Chap. 10.
- [11] M.R. Hakobyan, R.B. Alaverdyan, R.S. Hakobyan, Yu.S. Chilingaryan. Armenian Journal of Physics, **7**(1), 11 (2014).
- [12] M.R. Hakobyan, A.A. Ghandevosyan, R.S. Hakobyan, Yu.S. Chilingaryan. J. Contemp. Phys. (Armenian Academy of Sciences), **49**(5), 196 (2014).
- [13] M.R. Hakobyan, R.S. Hakobyan. J. Contemp. Phys. (Armenian Academy of Sciences), **46**(3), 116 (2011).